JMEPEG (2006) 15:627-631
DOI: 10.1361/105994906X150821

1059-9495/$19.00

Finite Element Simulation of Deformation Behavior in Friction Welding of Al-Cu-Mg Alloy

Li Qinghua, Li Fuguo, Li Miaoquan, Wan Qiong, and Fu Li

(Submitted December 29, 2005)

Friction welding is one of the most effective and widely used solid-state joining methods in modern industries. Plastic deformation of interface material is the essence of friction welding, and welding process parameters affect the welding quality greatly. To understand the friction welding process better, it is important to calculate the temperature, stress, and strain fields of welding interface material in the welding process. In this paper, continuously driven friction welding of Al-Cu-Mg alloy round bars that are commonly used in aerospace structures are calculated with the finite element method (FEM). FEM calculations and results are explained and discussed in much detail. For example, depending on experiments as reference, FEM results show that a temperature of 490 °C, which is below the low value of Al-Cu-Mg alloy melting point, is obtained at the end of 0.6 s of friction welding. During the whole process of friction welding, the calculated equivalent strains increase monotonously, and the equivalent strain at the center of circular section of interface material is the largest.

Keywords aluminum alloy, coupled simulation, finite element method (FEM), friction welding

1. Introduction

Friction welding is one of the most effective, energy-saving processes for solid-state joining of similar and dissimilar metals and alloys. It has the advantage of high joint integrity. The technology is widely used in high-tech industries, such as the aerospace industry. Friction welding is a process that involves complex thermodynamics, mechanics, and metallurgical qualities in the welding process. The plastic deformation of the interface material, which affects the welding process and joint quality greatly, is the essence of friction welding. However, it is difficult to measure the stress, strain, and other field parameters, thus it is very important to research these areas as well as other parameters of friction welding, including interface material plastic deformation. Finite element method (FEM) numerical simulation is a very powerful tool for simulating plastic deformation processes. Depending on the deformation field parameters calculated by FEM, the quality of the joint can be predicted and the welding processing parameters can also be optimized.

This work will focus on continuous driven friction welding. The rotational motion of the components to be welded has a constant rotation speed (n), and the other component to be welded is pushed toward the rotated part by sliding. The components are joined together under an axial friction pressure (P_f) for a certain friction time (t_f). The drive is then closed, and the rotary component quickly stops while the axial pressure is increased to a higher upsetting pressure (P_u), where it is kept for a predetermined time (t_u).

Li Qinghua, Li Fuguo, Li Miaoquan, and **Fu Li,** School of Materials Science and Engineering, Northwestern Polytechnical University, Xi'an 710072, China; and **Wan Qiong,** Hennan University of Science and Technology, Luoyang 471003, China. Contact E-mail: qinghual@nwpu.edu.cn.

In the friction welding process, a changing temperature will also cause the thermophysical parameters of the materials to fluctuate; instantaneously, the plastic deformation of the interface materials will change the heat-transfer space, boundary conditions, and energy transformation. So, the thermomechanical coupled finite element (FE) model was used to calculate the friction welding process. In the literature, just a few studies on numerical simulation of friction welding have been done, but most of them are not concerned with the thermomechanical coupled behavior or have not given detailed calculations. Sluzalec (Ref 1) established a FEM model computing the strain and stress fields in the welded components. Bendzsak (Ref 2) computed steady-state flow in friction welding using a numerical model. Recently, Fu (Ref 3) carried out a coupled deformation and heat flow analysis by FEM. D'Alvise (Ref 4) carried out a numerical code to simulate the inertia friction welding. This method helps to visualize the specific responses of the process easily and quickly and define the quality of the joint. Chen (Ref 5) developed his finite element modeling of friction stir welding, including thermal and thermomechanical analysis. Sahin (Ref 6) developed a computer program to simulate how the weld flashes occur in the welded joints with equal or different diameters. The aim of this study is to predict the temperature, stress, strain fields, and deformation in continuous driven friction welding by of the help of commercial FE software.

2. Energy Model and Boundary Conditions of Friction Welding Process

In friction welding, heat is generated into thermal energy by conversion of mechanical energy at the friction interface material. The friction surface is the symmetry surface of plastic deformation material. The heat flux density is assigned to the interface of the symmetry surface for similar material welding when calculating the deformation by FEM. To deduce the heat flux density model, a microannulus that has an inner diameter

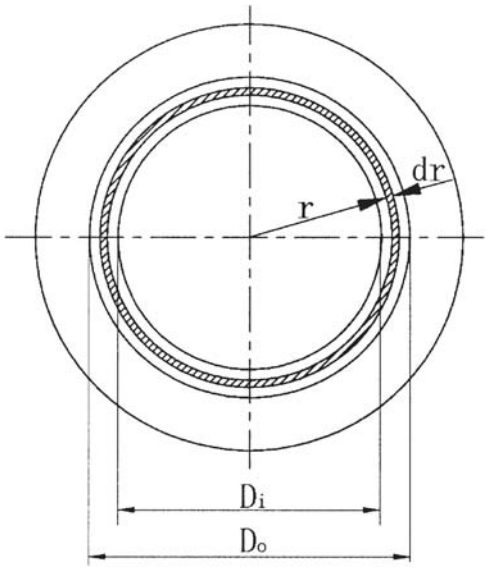

Fig. 1 Friction surface sketch

r and a width dr in the friction surface is defined in Fig. 1. The area of the microannulus is $ds = 2\pi rdr$. The friction on the microannulus is computed as $dF = 2\pi p_f ndr$. So, friction heat power in the microannulus area is written as follows:

$$dq = 4\pi^2 r^2 \mu p_f ndr \quad \text{(Eq 1)}$$

where P_f is the axial friction pressure, μ is the friction coefficient, and n is the axis rotation speed.

Depending on Eq 1, the integration of an annulus from inner diameter D_i to outside diameter D_o in the friction surface is the heat quantity of the area. The interface heat flux density model of continuous driven friction welding is then as follows (Ref 7):

$$q = \frac{4}{3}\mu p_f n\eta \frac{(R_o^3 - R_i^3)}{(R_o^2 - R_i^2)}\pi \quad \text{(Eq 2)}$$

where η is the friction heat efficiency, $R_i = D_i/2$, and $R_o = D_o/2$.

In analyzing the heat transfer on the surface of structure, the boundary conditions that are correlated to the temperature are defined in the following expressions:

$$T = \overline{T} \qquad \text{on the temperature boundary } \Gamma_T \quad \text{(Eq 3)}$$

$$\overline{q} = -\lambda \frac{\partial T}{\partial n} \qquad \text{on the heat flux boundary } \Gamma_q \quad \text{(Eq 4)}$$

The heat flux boundary conditions of friction welding process are included as follows:

(1) The heat flux boundary condition of friction surface:

$$q_f = \beta_f |\tau_f| |v_r| \quad \text{(Eq 5)}$$

where q_f is the heat flux density of friction power, β_f is the heat partition coefficient (in general, $\beta_f = 0\ 0.5$), τ_f is the friction stress of interface, and v_r is the sliding speed of the friction interface.

(2) Heat convention boundary condition:

$$q = h(T_s - T_\infty) \quad \text{(Eq 6)}$$

where h is heat convention coefficient, T_s is the surface temperature of part, and T_∞ is the external environment mediator temperature.

(3) Heat emission boundary condition:

$$q = \sigma\varepsilon(T_s^4 - T_\infty^4) \quad \text{(Eq 7)}$$

where σ is the Stefan-Boltzmann constant and ε is radiant efficiency.

3. Thermomechanical Coupled Analysis and FE Model

The temperature change of the deformation material will induce the physical property change. That will change the mechanical property of material, which will affect the deformation of the material. At the same time, the deformation process of material will affect the temperature distribution. In the material deformation analysis, the constitutive relationship of material and thermal strain will change by the influence of temperature field in the heat-transfer process. In analysis of the heat-transfer process, material deformation changes the heat-transfer space, boundary conditions, and energy transition during the deformation process.

A temperature field that acts on the deformation material will generate thermal deformation, and the thermal strain of the isotropic material is as follows:

$$\varepsilon_{Tij} = \begin{cases} \alpha\Delta T(i=j) \\ 0(i \neq j) \end{cases} \qquad (i, j = x, y, z) \quad \text{(Eq 8)}$$

where ε_{Tij} is the thermal strain component and α is the thermal expansion coefficient; ΔT is the numeric value of temperature change, and $\Delta T = T - T_r$, where T_r is the reference temperature.

Heat converted from deformation energy will affect the material temperature. So it should be taken into consideration in heat-transfer analysis, i.e.:

$$\omega_p = \alpha_p \overline{\sigma}\dot{\overline{\varepsilon}} \quad \text{(Eq 9)}$$

where ω_p is the heat source density that converted from plastic deformation energy, α_p is the heat conversion efficiency (in general, $\alpha_p = 0.9$~0.95; $\overline{\sigma}$, is equivalent stress, and $\dot{\overline{\varepsilon}}$ is equivalent strain rate).

In friction welding, the deformation process of joint material is accompanied with energy conversion and temperature change. Only when the deformation process coupled with the heat-transfer analysis is taken into account can FEM calculations simulate the actual welding process.

In the first step, experiments are done to get welding process parameters. In the experiments, 30 mm diameter Al-Cu-Mg

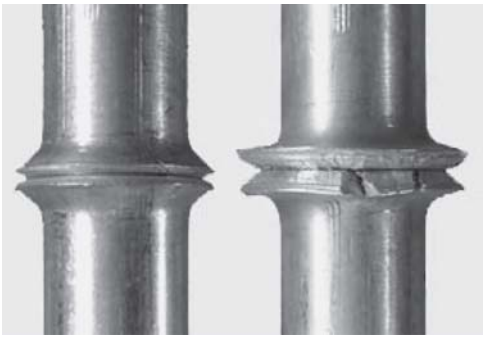

Fig. 2 Without upsetting specimen (left) and complete welding process specimen (right)

alloy AA2024 (T3) round bar specimens are joined by continuous drive friction welding; the appropriate welding process parameters are as follows: axis rotation speed is $n = 1450$ r/min, axial friction pressure is $P_f = 89.96$ MPa, friction time is $t_f = 4$ s, upsetting pressure is $P_u = 141.37$ MPa, and upsetting and keeping pressure time is $t_u = 6$ s. The left specimen in the Fig. 2 is from only friction for 4 s with no upsetting and keeping pressure; note the many cracks. The complete welding process specimen is displayed in the right side of Fig. 2; in addition to many cracks, there are deep splits in the flash. Because the plasticity of Al-Cu-Mg alloy is poor, when it deforms under high speed, cracks and splits occur easily during friction welding.

MSC.Marc software (MSC Software Corporation, Los Angeles, CA) is used to simulate the continuous drive the friction welding process. Because each side of the weld joint is the same, only one side of deformation sample was computed. The round bar sample has axial symmetry, and a two-dimensional (2D)-coupled FE model was established. The model dimension is 25 mm in length and 30 mm in width, which is equal to the diameter of the round bar samples; it was originally meshed into 3000 elements whose dimension is 0.5×0.5 mm, as shown in Fig. 3. The remesh function was selected in MSC.Marc to reduce the inaccuracy when the mesh distortion is too large.

4. Simulation Results and Discussion

Heat flux was loaded on the interface nodes of the FE model depending on Eq 1 at different radius; other welding process parameters are the same as in the experiments. When the pressure load was acted on the deformation boundary, it was easy to stop the calculation, due to the excessive deformation in the element when the iterative computation was not convergent. The displacement load that can be adjusted by the speed of motion load was acted on the interface, and the pressure roughly meets the experimental parameters.

The calculated deformation and temperature field of FE model at $t = 4$ s when the drive is closed are presented in Fig. 4. The calculated deformation is same as for the experiment specimens. The calculation deformation and temperature field of FE model at $t = 4.6$ s when the upsetting deformation is stopped are presented in Fig. 5. However, there are obvious errors in the calculation deformation. In this study, a two-dimensional FEM model is constructed, but it cannot calculate specimen radial cracks and splits. Thus, the difference in deformation between FEM calculation and experimental results can be large.

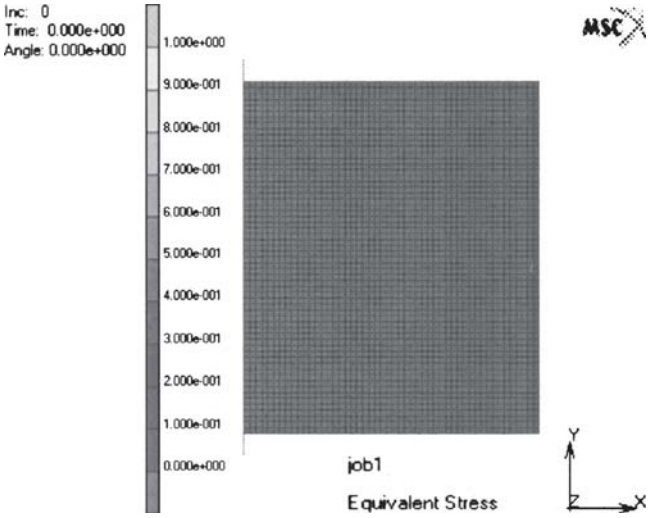

Fig. 3 Half FEM mesh of weld specimen

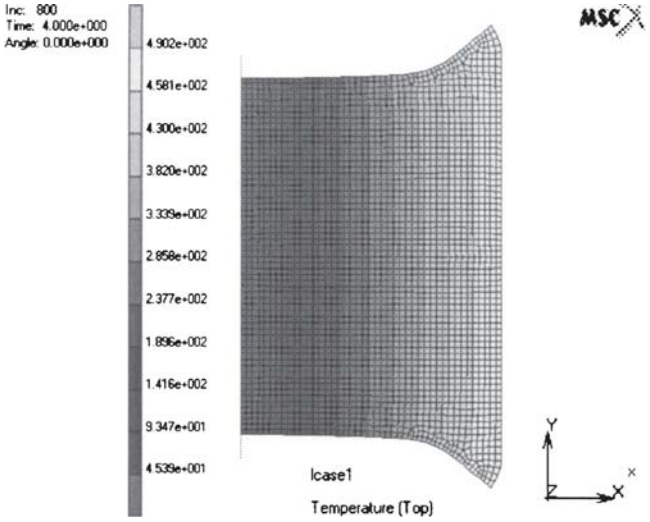

Fig. 4 Deformation and temperature contour bands at $t = 4$ s

The calculated axial friction welding pressure is presented in Fig. 6. The axial pressure is seen to fluctuate during the welding process. The calculated axial pressure gradually increases at the early welding stage, and then a pressure peak appears; after the peak point, the axial pressure gradually decreases. When the upsetting formation begins, the axial pressure rapidly increases and is maintained. At the beginning of welding, the interface temperature of the material is low, so the calculated axial pressure gradually increases with the motion until it reaches a peak point. When the pressure reaches its peak point, the interface temperature is high enough, and the material strength of the interface is reduced at this temperature, so that the deformation pressure is decreased.

Temperatures in different radius nodes of the welding interface that are picked from the FEM calculation are shown in Fig. 7. Because the maximum radius of friction interface has the maximum linear speed, heat generated there is the maximum and temperature rises faster than any others. It can be confirmed from the curves of $t = 0.1$ s and $t = 0.3$ s that the temperature is highest at the maximum radius of friction interface at the identical time. The heat will move from the high-

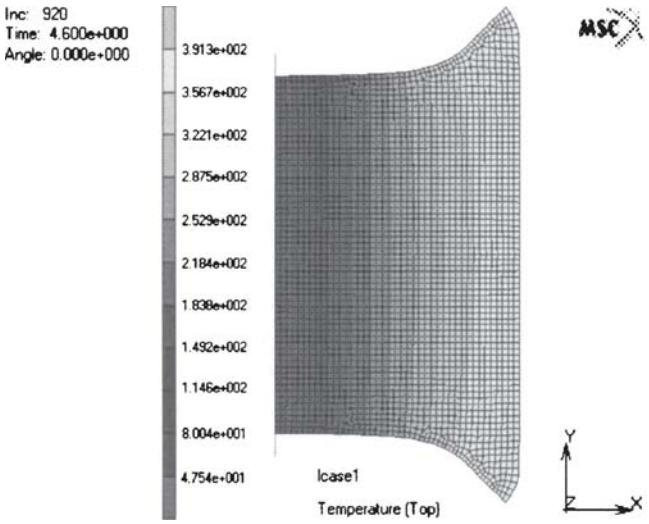

Fig. 5 Deformation and temperature contour bands at $t = 4.6$ s

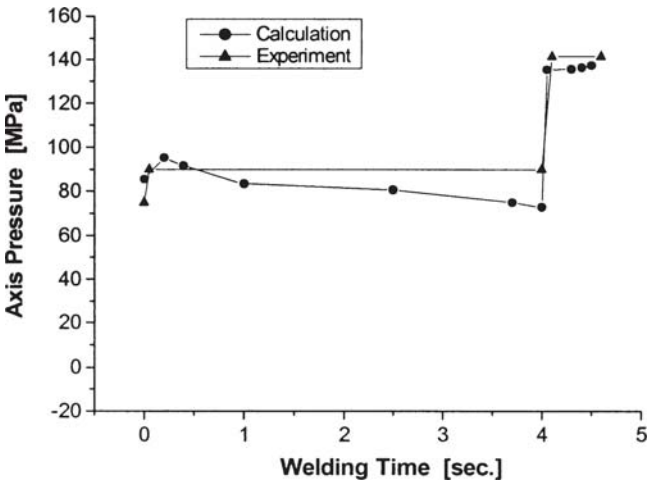

Fig. 6 Axial pressure

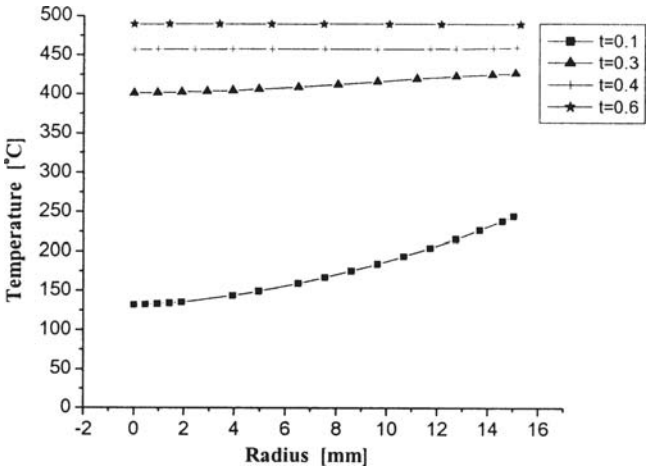

Fig. 7 Temperatures at different radii of welding interface

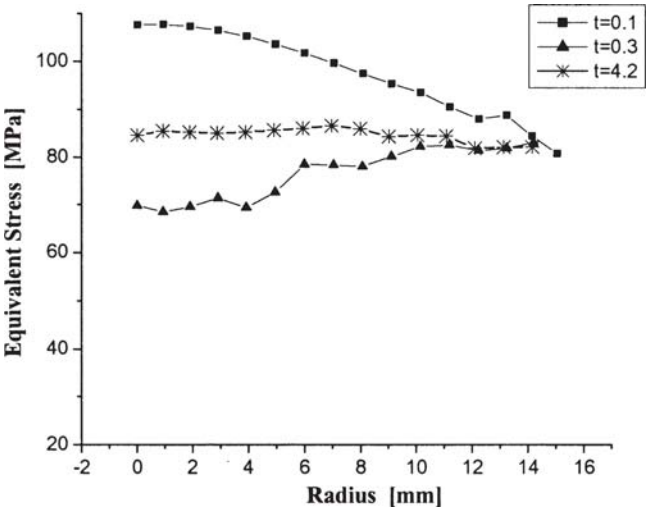

Fig. 8 Welding interface equivalent stress along the radius at different welding times

temperature area to the low-temperature area when there are temperature differences, so the interface temperature is gradually uniform, shown as the curve $t = 0.4$ s in Fig. 7. The temperature curve of $t = 0.6$ s is 490 °C, which is lower than the low value of the melting point in Al-Cu-Mg alloy (502-638 °C); it rises slightly compared with that of the $t = 0.4$ s curve. After $t = 0.6$ s, the calculated interface temperature is almost the same as the $t = 0.6$ s curve and there is little fluctuation. This indicates that the interface energy is in dynamic balance.

During the early welding stage, the interface temperature is low, the deformation equivalent stress is large, and the temperature at small inner radius is lower than that at the large outer radius. So, the interface's inner equivalent stress is greater than the outer equivalent stress. It is indicated by the $t = 0.1$ s curve in Fig. 8. The $t = 0.3$ s curve in Fig. 8 shows that the equivalent stress at the large outer radius of the interface area is higher than that of the small inner radius. This is correct because the interface temperature reaches the starting forge temperature and materials begin to motion to the outside and turn to the flash, so the equivalent stress at the large outer radius of the interface area is higher than that of small inner radius. The equivalent stress of the $t = 4.2$ s curve in Fig. 8 is almost a horizontal line, and the right end is a little low, so the flash is easier to deform than the inner material during the upsetting when the drive is stopped.

The calculated equivalent strain of welding interface material at radii of 0, 5, and 13 mm during the process are shown in Fig. 9. The figure shows that the equivalent strain gradually increases and reaches the maximum value when the material stops upsetting deformation. It can be seen in Fig. 9 that the equivalent strain of the small inner radius is larger than that of large outer radius, so the interface material from the inside motions to the outside and turns to the flash. The keeping pressure stage when material is not being deformed is not at the key research stage, and the subsequent process has not yet been calculated.

5. Conclusions

Depending on the experimental parameters, a 2D thermo-mechanical coupled FE model was established to calculate continuous driven friction welding Al-Cu-Mg alloy bars using

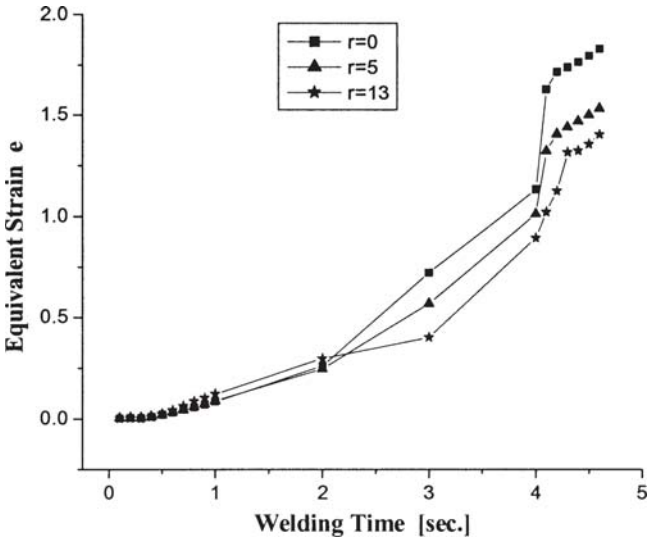

Fig. 9 Welding interface equivalent strain at radii of 0, 5, and 13 mm at different welding times

MSC.Marc. The temperature field, stress field, strain field, and deformation of HAZ materials were calculated. The calculated deformation is the same as the experimental specimen before the drive is completed. Because the 2D FE model cannot calculate radial cracks and splits, obviously there are some differences between the calculated deformation and experimental results when upsetting occurs.

The calculation results indicate that temperature of interface material tends to be same when the welding time is 0.4 s. The temperature is 490 °C at 0.6 s, which is lower than the lowest melting point value of Al-Cu-Mg alloy. After that time, the calculated temperature is nearly constant. This indicates that the interface energy is in dynamic balance.

The calculated equivalent strain of welding interface material is gradually increased monotonously during the welding process, and the equivalent strain reaches a maximum value when the materials stop upsetting deformation. The inner interface material moves to the outer surface and turns to flash, and the calculations confirm that the equivalent strain of the small inner radius is greater than that of the large outer radius.

Acknowledgments

Special thanks are due to National Natural Science Foundation of China for supplying research funding. Thanks also to Shannxi Province Engineering Center of Friction Welding Technology for supplying the experimental apparatus.

References

1. A. Sluzalec, Thermal Effects in Friction Welding, *Int. J. Mech. Sci.,* 1988, **32**(6), p 467-478
2. G.J. Bebdzsak, T.H. North, and Z. Li, Numerical Model for Steady-State Flow in Friction Welding, *Acta Mater.,* 1997, **45**(4), p 1735-1745
3. L. Fu and L. Duan, The Coupled Deformation and Heat Flow Analysis by Finite Element Method During Friction Welding, *Weld. Res.,* 1998 (Suppl), p 202-207
4. L. D'Alvise, E. Massoni, and S.J. Walløe, Finite Element Modelling of the Inertia Friction Welding Process Between Dissimilar Materials, *J. Mater. Process. Technol.,* 2002, **125-126,** p 387-391
5. C.M. Chen and R. Kovacevic, Finite Element Modeling of Friction Stir Welding—Thermal and Thermomechanical Analysis, *Int. J. Machine Tools Manuf.,* 2003, **43,** p 1319-1326
6. M. Sahin, Simulation of Friction Welding Using a Developed Computer Program, *J. Mater. Process. Technol.,* 2004, **153-154,** p 1011-1018
7. L. Fuguo, N. Lei, L. Qinghua, and D. Ligu, Microstructure Simulation and Prediction of IN-718 Superalloy in Inertia Friction Welding, *Trans. China Welding Inst.,* 2002, **23**(1), p 30-33, in Chinese